2013/3/14

海岸環境における鋼の腐食挙動におよぼす表面処理の影響

広島大学名誉教授　中佐啓治郎

この研究は，エジプトからの留学生　MANAL GOMAA MAHMOUD OSMAN ALI（マナル ゴマー マーモウド オスマン アリ）さん（通称 Manal さん，アレキサンドリア海洋水産国立研究所）が，博士課程で行ったものです。この研究の遂行とまとめには，当時，広島大学ベンチャービジネスラボラトリ主任：長野博夫教授の絶大なるサポートがありました。

公表論文

1. Evaluation of Atmospheric Corrosion Resistance in Simulated Seaside Environment for Various Kinds of Stainless Steels with Different Surface Treatments, Manal Mahmoud, Jun Itoh, Hiroo Nagano and Keijiro Nakasa, 材料と環境, 第 53 巻，第 2 号 (2004) pp. 69-75.

2. Effect of Gas Nitriding on Hydrogen-Induced Cracking on Pure Iron and Cr-Mo Steel, Manal Mahmoud Gomaa, Keijiro Nakasa, Masahiko Kato, Rongguang Wang, Yosiaki Murakami, Proceedings of the Third International Conference on Environment Sensitive Cracking and Corrosion Damage (2004) pp. 56-60. (August, Qingdao, China)

3. Atmospheric Corrosion Resistance of Stainless Steels in Laboratory Accelerated Seashore Environment, Hiroo Nagano, Manal G. Mahmoud and Keijiro Nakasa, Proceedings of the Third International Conference on Environment Sensitive Cracking and Corrosion Damage (2004) pp. 168-172. (August, Qingdao, China)

4. Rust formation Behavior on Carbon and Weathering Steels in Wet/Dry Cycles with and without Na_2SO_4 Solution Spraying Combining NaCl or $MgCl_2$ Solution Dripping, Manal G. Mahmoud, Jun Itoh, Hiroo Nagano and Keijiro Nakasa, 材料と環境，第 54 巻，第 6 号（2005) pp.268-274.

5. Influence of Ultraviolet Light Irradiation on Corrosion Behavior of Weathering Steel with and without TiO_2-Coating in 3 mass% NaCl Solution , Manal G. Mahmoud , Rongguang Wang, Masahiko Kato, Keijiro Nakasa, Scripta Materialia, 53(2005), pp.1303-1308.

Manal さんの博士論文の概要を次ページ以降に示します。

STUDY ON EFFECT OF SURFACE TREATMENTS ON CORROSION BEHAVIOR OF STEELS IN ACCELERATED SEASHORE ENVIRONMENT

Chapter 1: Background and Objective of the Research

Corrosion is destructive attack of electrochemical reaction on metal with surrounding environments. There are many types of corrosion including general corrosion, galvanic corrosion, pitting corrosion, crevice corrosion, stress corrosion, and biological corrosion that occur in various environments. Marine environment is the one of the most aggressive corrosion environments. Weathering steels and stainless steels are the most common steels used in this environment due to the formation of protective and passive layer.

There are so many researches to investigate the corrosion and to protect corrosion. Surface modification is one of the effective methods to prevent corrosion. However there are some problems remain unsolved that will be treated in chapter 2, chapter 3, chapter 4, and chapter 5. The purpose of present research is to investigate the effect of surface treatments on corrosion behavior of different kind of steels in accelerated seashore environment. The results obtained are summarized as follows:

Chapter 2: Effect of Wet/Dry Cycles on Rust Formation Behavior on Carbon Steel and Weathering Steel in NaCl and $MgCl_2$ Solution Dripping

Formation behavior of protective rust that can be considered as (nature coat) on weathering is not clear. Therefore development of an accelerated corrosion test using short interval wet/ dry cycles to simulate marine atmosphere will be helpful to get quick and clear information about effect of each parameter on the protective rust formation. The purpose of the research in this chapter is to study the initial stage of rust formation behavior on weathering and carbon steels under controlled wet and dry cycles in laboratory accelerated marine atmosphere.

Weathering steel (SMA490) and carbon steel (SM490A) are used in this study. The samples were put in wet/dry cyclic corrosion test chamber for 14 and 28 days with and without spraying of Na_2SO_4 solution combined with dripping of NaCl or $MgCl_2$ solution as schematically shown in Fig (1).

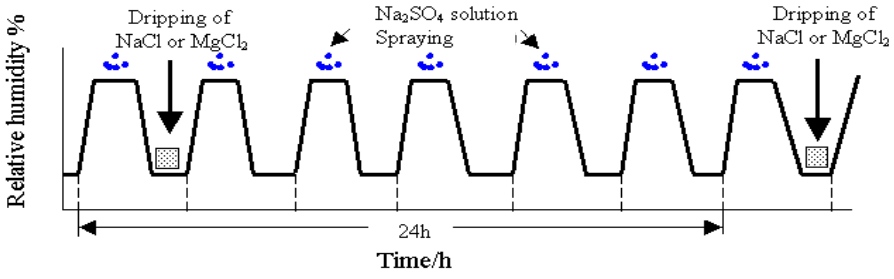

Fig.1 wet/dry cycles in accelerated corrosion test to simulate marine atmospheric corrosion.

After the test periods were ended the weight loss, analysis of rust, and surface potential measurement were carried out. As shown in Figs.2 and 3 for both steel the weight loss curves with spraying of Na_2SO_4 are straight indicating that the protective rust is not formed. On the

other hand, the rate of weight loss without spraying decrease with time suggested that the protective rust is being formed with time.

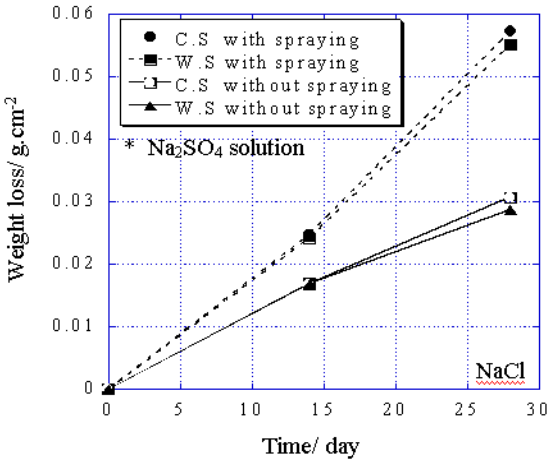

Fig.2 Weight losses for carbon steel (C.S) and weathering steel (W.S) with dripping of NaCl solution with or without spraying.

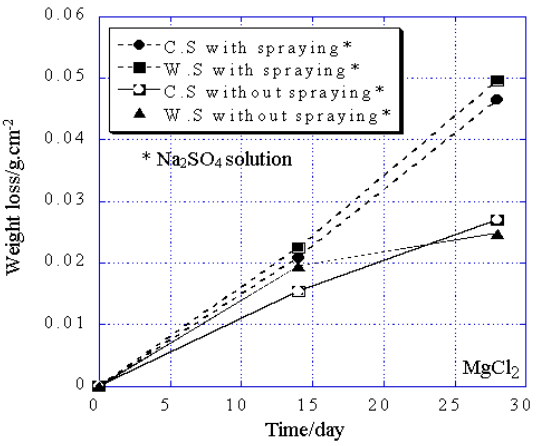

Fig.3 Weight losses for carbon steel (C.S) and weathering steel (W.S) with dripping of $MgCl_2$ solution with or without spraying.

According to XRD results the higher percentage of X-ray amorphous substance that may contain nano size goethite (protective rust) was detected in the rust without spraying than with spraying for both steel either with dripping of NaCl or $MgCl_2$. Moreover as shown in Figs.4 and 5 without spraying dense and dark rust, are formed, while with spraying the rusts are all porous.

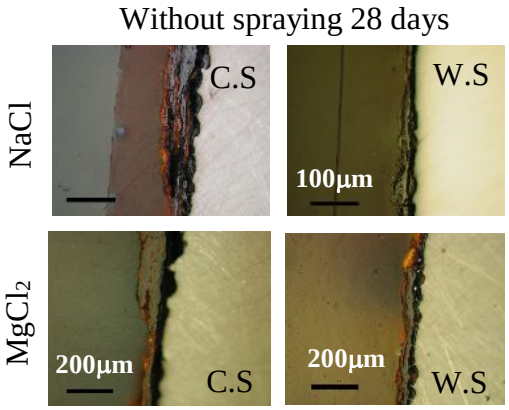

Fig.4 Rust layers formed for the exposure of 28 days without spraying of Na_2SO_4 for carbon steel (C.S) and weathering steel (W.S) with dripping of NaCl and $MgCl_2$.

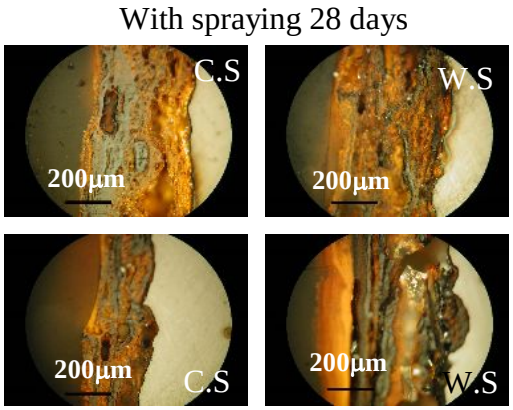

Fig.5 Rust layers formed for the exposure of 28 days with spraying of Na_2SO_4 for carbon steel (C.S) and weathering steel (W.S) with dripping of NaCl and $MgCl_2$.

The surface potential measured by Kelvin probe also showed that the rusts of weathering steel and carbon steels after 28 days exposure without spraying was more protective than with spraying. As shown in Figs.6 and 7 without spraying the values of the minimum surface

potential after wetting is higher than –0.2V vs Ag/AgCl satd., which is the state of passivity. However with spraying the values of minimum surface potential is much lower than this value.

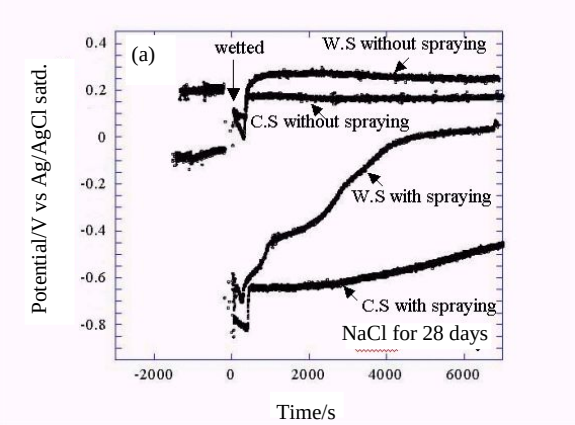

Fig.6 Surface potential for C.S and W.S with and without spraying with dripping of NaCl for 28 days.

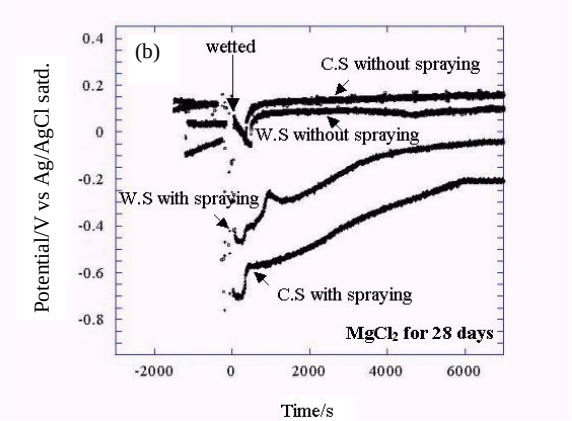

Fig.7 Surface potential for C.S and W.S with and without spraying with dripping of $MgCl_2$ for 28 days.

Another proof that the protective rust is being formed without spraying is that the surface potential of both steel with dripping of either NaCl or $MgCl_2$ are close to those steel exposed in real mountainous environment for 17 years (where the protective rust is easy to be formed).

Chapter 3: Effect of Ultraviolet Light Irradiation and TiO_2-Coating on Corrosion Behavior of Weathering Steel in 3% NaCl Solution

The protective rust is semiconductor substance that affected by UV-light. In addition it is known that the TiO_2 is n-type semiconductor. When the semiconductor substances absorb the UV-light whose energy is higher than the band gab energy photoelectron and positive holes can be generated. The photo-electrochemical reaction between positive holes, electron, oxygen and water produce active oxygen species $O_2^{\bullet -}$ (eqn.1and 2), $OH^{\bullet}$ radical, H_2O_2, *etc.*. These can affect the corrosion behavior either by acceleration or inhibition.

$$2H_2O + 4h^+ \rightarrow O_2 + 4H^+ \quad (1)$$

$$O_2 + 2e^- \rightarrow 2O^- \ (O_2 + e^- \rightarrow O_2^{\bullet -}) \quad (2)$$

Since the weathering steel usually use as outdoors structure materials and the sun radiation contain severe UV-light especially in marine atmosphere. Therefore the purpose of the research in this chapter is to is to investigate the corrosion and rust formation behavior of weathering steel with and without TiO_2-coating under UV-light in polarization, dipping and dropping test using sodium chloride solution.

TiO_2 was sputtered on weathering steel (SMA490W) using RF magnetron sputtering apparatus. Polarization, dipping and dropping test were carried out in 3% NaCl solution in dark and UV-light. The potentiodynamic polarization test was carried out in order to confirm the photoelectochemical reaction on the TiO_2-coat and rust. The results shown in Fig.8 indicate that for samples without coating, the curves are almost the same in dark and under UV-light.

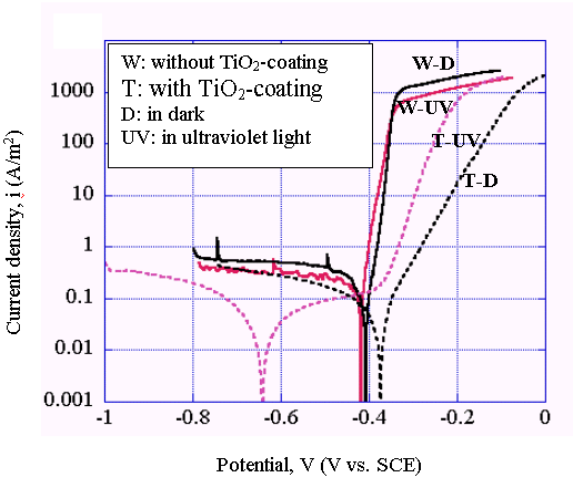

Fig.8 Polarization curves of the specimens without TiO_2-coating in dark (W-D), without TiO_2-coating under UV-light (W-UV), with TiO_2-coating in dark (T-D), and with TiO_2-coating under UV-light (T-UV).

On the other hand the corrosion potential of TiO_2-coat specimens in dark is a little more positive than those of specimens without coating and considerable decrease in anodic current density is observed indicating the shielding effect of TiO_2-coat. In contrast, under UV-light, the corrosion potential of TiO_2-coated specimen shifts to much more negative value with a considerable decrease in anodic current density which is explained by the migration of photoelectrons generated under UV-light to the interface, and they prevent the dissolution of iron, which mean cathodic protection effect. The polarization tests were carried out again on all the specimens used for first polarization tests. As shown in Fig.9 for the specimen without TiO_2-film a little larger negative shift of corrosion potential occurs under UV-light than in dark, which proves that the rust has a nature of n-type semiconductor like TiO_2 film.

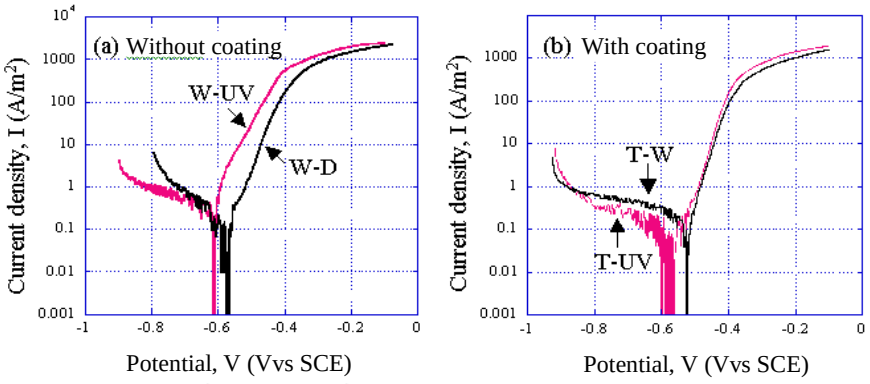

Fig.9 Repolarization curves obtained by repeating the polarization test for the specimens (a) without coating, and (b) with TiO_2-coating.

In the dipping test, as shown in Fig.10 the weight loss was lower in the steels with TiO_2-film than in the steel without film both in dark and UV-light due to the shielding effect of TiO_2-coating. The UV-light increased the weight loss of both steels with and without TiO_2 film within 2765ks (32 days), which will be explained by the promotion of corrosion and rust formation due to the active oxygen generated by photo-electrochemical reaction in UV-light.

This result also suggests that the TiO_2 film has the same effect as the rust on the specimens without coating. The thickness of rust on cross-section shown in the same Fig.10 corresponds well to the weight loss of each sample after dipping of 2765ks (32 days).

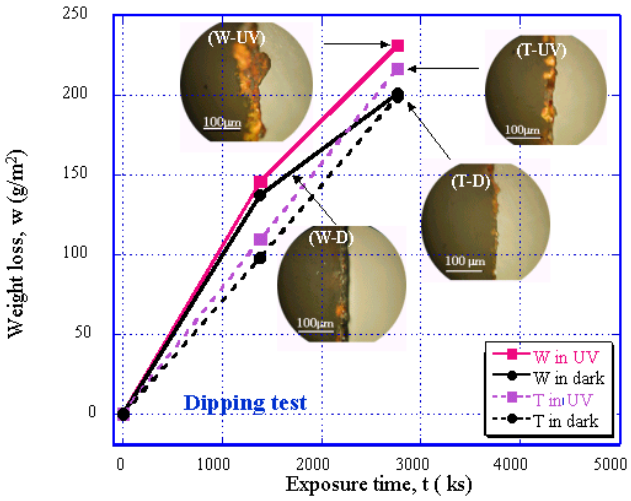

Fig.10 Weight loss and cross section view of the specimens in dipping test without coating in dark (W-D), without coating under UV light (W-UV), with TiO_2-coating in dark (T-D), with TiO_2-coating under UV light (T-UV).

According to XRD pattern of powdered rust on the specimens after dipping test of 32 days the higher peak from stable goethite (α-FeOOH) and lower peak from Fe_3O_4 were detected in dark than in UV-light. Perhaps active oxygen suppressed the transformation from hydroxide to α-FeOOH (protective rust) but rather promote the reaction from hydroxide to Fe_3O_4 that may be one of the reasons for the lower corrosion rate in dark than in UV-light shown in Fig.10.

In dropping test the UV-light decreased the weight loss of the specimens with and without TiO_2 film when the test period is 3456ks (40 days) as shown in Fig.11. The photo-electrochemical reaction of semiconductive oxides formed under higher oxygen than in dipping test might have promoted the protective nature of the rust. This can be confirmed from cross section views of the specimens after 32 days dropping test shown in Fig.12. As shown the rust is denser and the amount of dark region is greater in the rust in UV-light than in dark.

In addition UV-light not only promote the formation of Fe_2O_3 according to X-ray data but it seems also promote the formation of nano sized goethite including amorphous phase, which cannot be detected by X-ray analysis. These nano-sized goethite and amorphous phase are considered to prevent the weight loss after 1382(16 days) in Fig.11, although the detailed rust formation mechanism due to active oxygen is not clear.

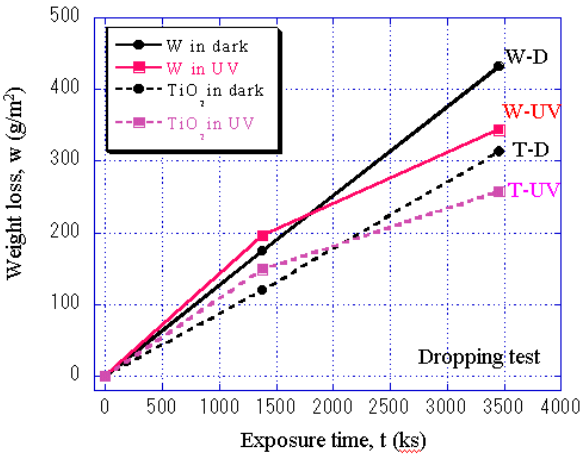

Fig.11 Weight loss of the specimens in dropping test without coating in dark (W-D), without coating under UV light (W-UV), with TiO_2-coating in dark (T-D), with TiO_2-coating under UV light (T-UV).

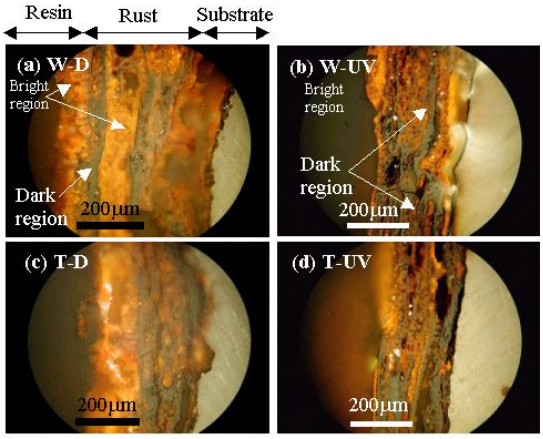

Fig.12 Rust layers formed on the specimens in dropping test after 2765 ks (32 days). (a) without coating in dark (W-D), (b) without coating under UV-light (W-UV), (c) with TiO_2-coating in dark (T-D), (d) with TiO_2-coating under UV-light (T-UV).

Chapter 4: Effect of Surface Finish on Atmospheric Corrosion Resistance in Simulated Seaside Environment for Stainless Steels

Stainless steel is an alloy of great interest in various applications where materials with high corrosion resistance are required due to its passive film formation. This passive film is affected by the chemical composition and surface treatment. Therefore the research in this chapter is composed of two items. First is to evaluate pitting corrosion resistance for different grades of stainless steels that belongs to different classes such as austenitic (SUS 304, SUS 316, SUS 316L), ferritic (SUS 444, SUS 445J2), and duplex (SUS 329J4L, SUS 329J3L). The second is to investigate the effect of surface treatments commercially prepared for conventional stainless steels.

The surface treatments of austenitic, ferritic, duplex stainless steels that used in this study are shown in table 1

Table 1 Different surface treatments studied.

	Surface treatment		**Surface treatment**
No.1 (a)	Plate is hot rolled, annealed and pickled. It is featured by a dull and slightly rough surface.	No.2B (c)	No.2D finish is followed by a subsequent light skin pass cold rolling with polishing rolls. It is brightened.
No.2D (b)	A mat finish with grit abrasive after being cold rolled, annealed and pickled.	No.4 (d)	A ground finish without any acid pickling.

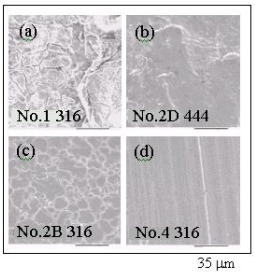

Pitting potential measurements in 3% NaCl solution and accelerated corrosion test were carried out for evaluation of corrosion resistance. Fig. 13 shows the anodic polarization curves for stainless steels with surface finish No.4. as an example. From this kind of curves pitting corrosion of stainless steels was evaluated by the pitting potential, where it is termed

the potential at 10 μA /cm^2 or 100 μA /cm^2, in the anodic polarization, and illustrated in Fig. 14.

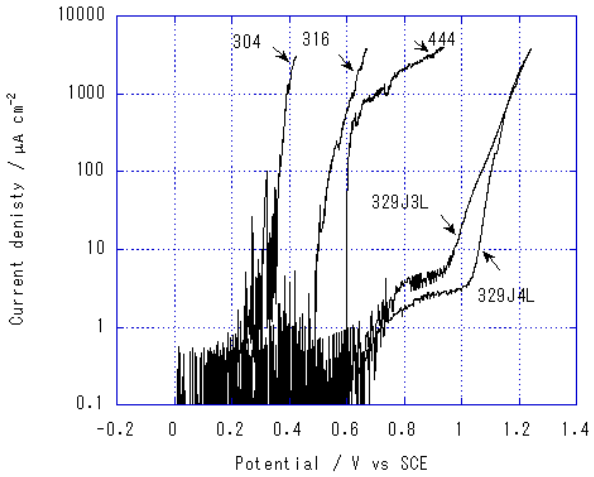

Fig.13 Anodic polarization curves in 3% NaCl solution for stainless steels with surface finish No.4.

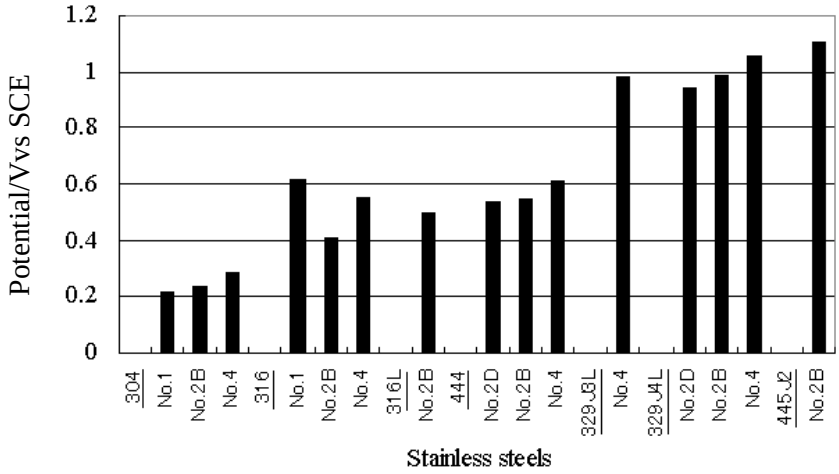

Fig.14 Evaluation of surface treatments by pitting potential at 10 μA/cm^2.

As shown in Fig.14 pitting corrosion resistance, which corresponds to higher value of pitting potential, increased in the following order of SUS 304< SUS 316< SUS 316L< SUS 444< SUS 329J3L< SUS 329J4L< SUS 445J2. This is due to the increase in the Cr, Mo, and N content. Moreover it is concluded that the chemical composition plays a more important role on the corrosion resistance of the alloys than surface treatments

The surface of the sample was observed by SEM before and after the polarization measurements. As shown in Fig.15 the surface finish No.4 is the best surface concerning the pitting resistance that pits were formed not at grain boundaries but along the line of grinding, and pitting attack is smaller than No.2B and No.1. In general we can conclude that the order of surface treatments to pitting corrosion resistance in 3% NaCl solution is No.4(polishing)> No.2B (Brighten) > No.2D (dull) or No.1(pickled). This could be attributed to the fact that roughness and homogeneity of surfaces influence corrosion resistance, particularly localized corrosion resistance of stainless steels. Surface finish No.4 has least irregularity and defects, which leads to completion of uniform passive film.

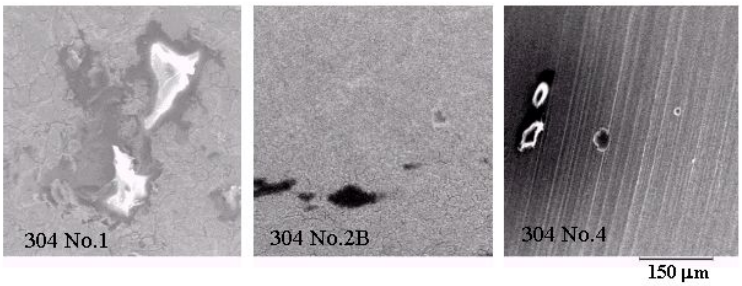

Fig.15 SEM images of SUS 304 No.1, No.2B, and No.4.

In accelerated corrosion test, after the test was ended the appearance of the surface was observed using an optical microscope. Austenitic stainless steels as SUS304, SUS316, and SUS316L had general corrosion, pitting corrosion or both types of corrosion attack. No.4 surface treatments of austenitic stainless steels maintained almost passivity although showing some pits. No pitting or general corrosion occurred on SUS329J4L and SUS444No.4. For ferritic stainless steels, SUS445J2 No.2B and SUS444No.4 were highly resistant.

In addition right after taking out the sample from the test chamber, the surface potential was measured for the center spot on the surface of the sample. The measurement was made twice i.e., the first was before the rust was taken away and the second was after the rust was taken away and washed in $MgCl_2$ solution followed by wiping of residual solution on the surface by filter paper. Fig.16 illustrates the surface potentials at the times before and after washing. As shown the stainless steel with pits at the center spot tended to lower the surface potential more negative after washing. The drop of V_{kp} is attributed to keeping the electrolyte inside the pores of the pits. When the stainless steel has no corrosion, no difference has been appeared in the V_{kp} before and after washing. On the other hand, the surface potential of samples which had general corrosion shifted to more positive values after washed and wiped with filter paper. This may be due to repassivation of corroded surface by the cleaning procedure. Therefore, the V_{kp}, makes it possible to know whether the stainless steel is in passivity or in corrosion. These behaviors of pitting corrosion in the accelerated seashore environment are almost the same as the behaviors in the anodic polarization tests in 3% NaCl solution. Both tests showed that the stainless steels with high corrosion resistant in seashore environment were SUS445J2, SUS329J4L and SUS329J3L, while SUS304, SUS316 and SUS316L steels were susceptible to corrosion.

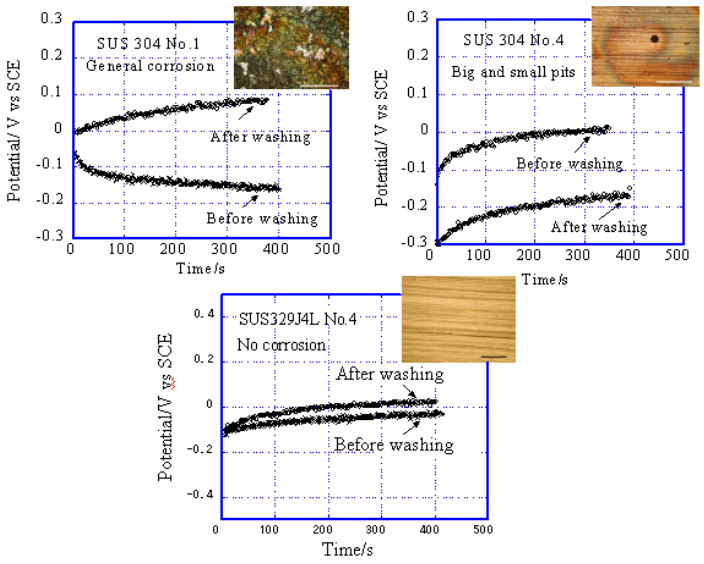

Fig.16 Kelvin potential with time and optical microscope images at the center spots.

Chapter 5: Effect of Gas Nitriding on the Corrosion and Hydrogen Damage of Steels

Hydrogen damage is another serious problem in the field of the corrosion as when the steel exposed to marine environment the corrosion occurred. The hydrogen atoms from the cathodic reaction of corrosion can enter to the structure causing the hydrogen damage. To prevent the hydrogen entry addition of alloying element is effective method but it is expensive. Another method is the surface modification like coating. However, the coating is not so effective due to its delamination. Gas nitriding seems to inhibit corrosion and hydrogen entry because the delamination of modified layer is difficult to occur due to continuous interface microstructure. Therefore the purpose of present research is to examine the effect of gas nitriding on the corrosion, hydrogen entry and hydrogen damage of steels.

The materials used in this study are pure iron (JIS: SUYP1), weathering steel (JIS: SMA490W), and annealed Cr-Mo steel (JIS: SCM435). After the samples were cut and polished they were applied to the gas nitriding. Corrosion test was carried out for weathering steel and pure iron in 3% NaCl solution. However hydrogen-charged test was carried out for Cr-Mo steel and pure iron in 0.5kmol/m^3 H_2SO_4 aqueous solution. Fig.17 (a) and (b) shows SEM image of cross section for weathering steel and Cr-Mo steel that were gas nitrided at 773K for 14.4ks. The gas nitride layer is about 10μm and 2μm respectively. The nitride layer according to the XRD is composed of ε iron-nitride (Fe_3N) and ζ iron-nitride (Fe_2N). The existence of diffused and dissolved nitrogen atoms in the lattice or grain boundary is confirmed from measurement of the distribution of hardness in the depth for the gas nitrided specimens shown in Fig.18. The hardness is larger near the surface both for pure iron and Cr-Mo steel, and it gradually decreases with increasing depth. So the reason for the increase in hardness in this region (<20μm) is attributed to diffusion layer.

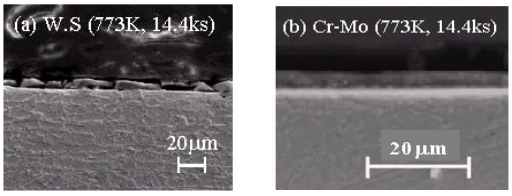

Fig.17 Micro-structures of weathering steel (W.S) (a), and Cr-Mo steel (b) after gas nitriding at 773K for 14.4ks.

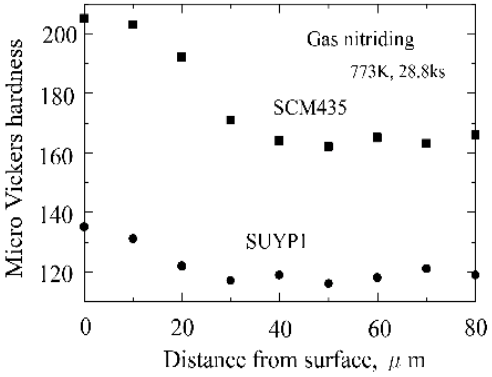

Fig.18 Cross-sectional distribution of hardness near specimen surface.

Effect of gas nitriding on the corrosion behavior of weathering and Cr-Mo steels is shown in Fig.19 and 20 respectively. As shown the natural corrosion potential shifts to positive direction, which means that the corrosion resistance is increased by gas nitriding.

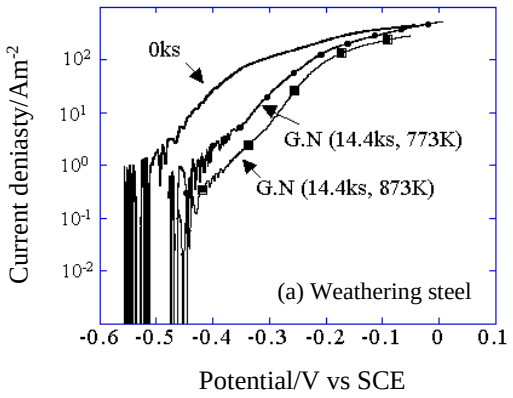

Fig.19 Polarization curves of specimens with and without nitriding of weathering steel.

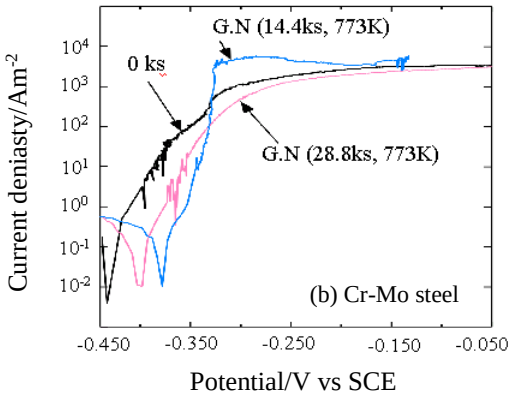

Fig.20 Polarization curves of specimens with and without nitriding of Cr-Mo steel.

In order to examine the effect of gas nitrinding both of thin nitride layer and diffusion layer on blister formation behavior in Pure iron and Cr-Mo steel the surface and cross section of the three kind of specimens (without gas nitriding, gas nitrided, gas nitrided but the surface is polished) were observed by an optical microscope, and the number, diameter and depth of the blisters were measured. Fig.21 shows the blister growth with the charging time of 173ks (48h) for the Cr-Mo steel specimens as an example. From these kinds of photographs the histogram of blister size are obtained as shown in Fig. 22. The number of large blisters is smaller on the surface of gas-nitrided specimen than the original specimen, and the numbers of blisters are larger but the size is smaller for the surface-polished specimen than original specimen.

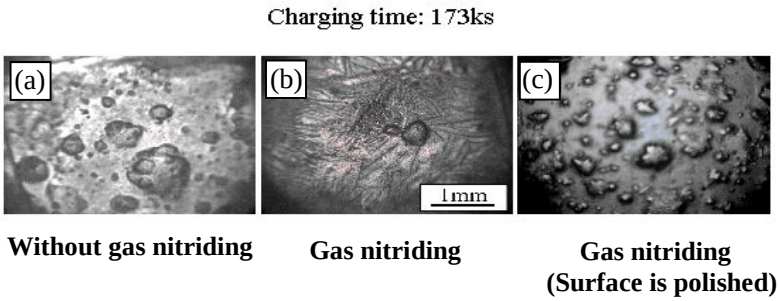

Fig.21 Blisters formed on the surface of Cr-Mo steel specimens after hydrogen-charging for 173ks.

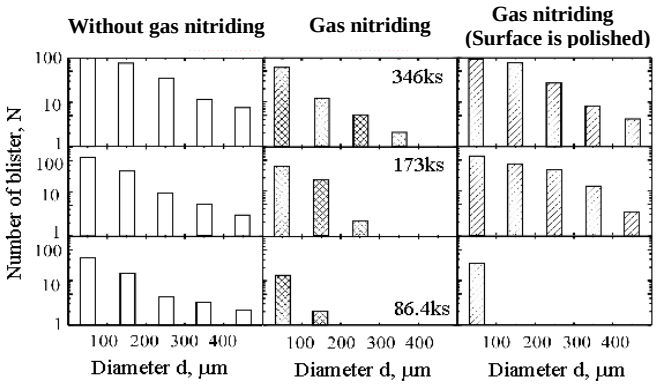

Fig.22 Histogram between diameter and numbers of blisters in Cr-Mo steel.

Fig.23 shows the examples of cross sectional views of the specimens with and without gas nitriding. From these photographs at various parts of specimen, maximum depth of blister in each photo was measured. Fig.24 shows the relationship between hydrogen-charging time and maximum depth of blisters. Blisters exist at more shallow position for gas-nitrided specimen or surface polished specimen than original specimen. This means that the nitriding prevents the hydrogen entry or diffusion of hydrogen and limit the damage near surface. The results for pure iron are also shown in Fig.24 by dotted circle. It is clear that much longer charging time is necessary for blister formation for Cr-Mo steel specimens both original and gas-nitrided specimen than for pure iron. The reason will be that the alloying elements, Cr and Mo, decrease the diffusion velocity of hydrogen by the distortion of the lattice of matrix.

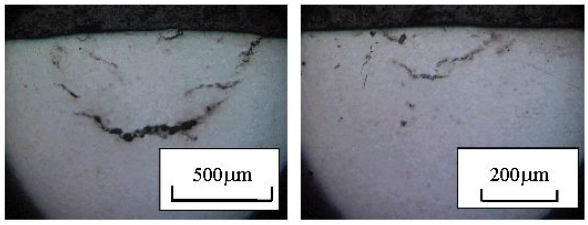

Without gas nitriding (173ks) Gas nitriding (347ks)

Fig.23 Cross-sectional view of blisters in Cr-Mo steel specimens.

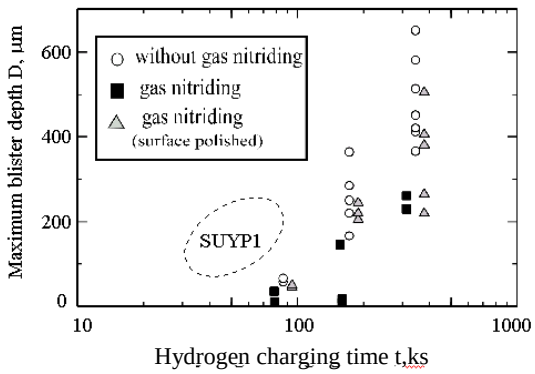

Fig.24 Relationship between hydrogen charging time and maximum blister depth for Cr-Mo steel.

Delay of blister formation is observed for gas-nitrided specimen compared with the specimen gas-nitrided but surface is polished, which shows that even a thin nitride layer has the resistance to hydrogen entry into specimen. Nitrogen diffusion region under nitride layer has some resistance to hydrogen entry, which is observed by the comparison between original specimen and the specimen gas-nitrided but surface is polished.

In order to confirm the inhibition of hydrogen entry due to gas nitriding the hydrogen evolution amount was measured using a gas chromatography. Fig.25 (a) and (b) show the hydrogen evolution curves obtained for pure iron and Cr-Mo steel in original and gas-nitrided specimens that was hydrogen charged for 86.4ks respectively. The area under these curves corresponds to the total amount of absorbed hydrogen in the specimens. As shown the area of gas-nitrided specimen is smaller than that of the specimen without nitriding, which means the hydrogen entry is suppressed by gas nitriding.

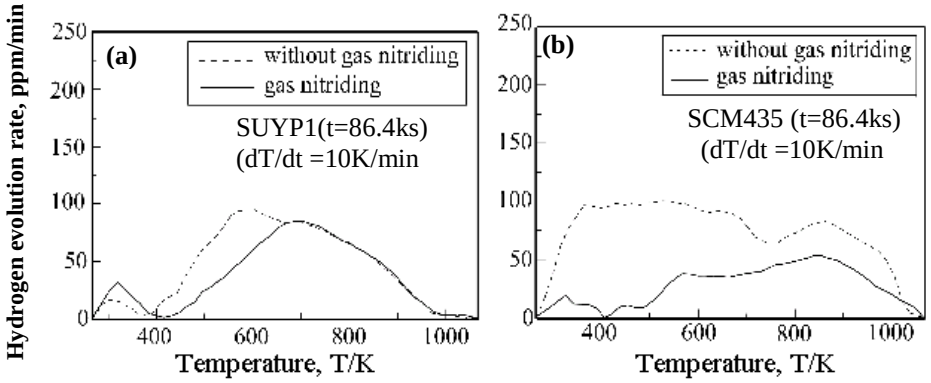

Fig.25 Relationship between temperature and hydrogen evolution rate in (a) pure iron and (b) Cr-Mo steel.

The estimated mechanism of inhibition of hydrogen entry and hydrogen damage by gas nitriding is illustrated in Fig.26. For original specimen (Fig.26 (a)), hydrogen atoms adsorbed on specimen surface enter into metal passing through the interstitial positions of lattice. Alloying elements such as Cr and Mo decrease the diffusion velocity of hydrogen by the distortion of lattice of matrix. Various defects, such as vacancy, dislocation, grain boundary, will trap hydrogen atoms and delay the diffusion of hydrogen. When certain amounts of hydrogen atoms gather at such a trap site, the precipitated hydrogen gas with high-pressure separates the matrix and form a void. The void grows taking ellipsoidal shape parallel to the surface of specimen and forms a blister. During gas-nitrided process, nitrogen atoms diffuse from surface and the nitride layer is formed on specimen surface. At the same time nitrogen atoms dissolve into lattice taking interstitial position, gather around dislocations and grain boundary. In addition, Cr- or Mo-nitrides with small size can be formed under nitride layer. Nitrogen atoms also gather along carbide- or nitride-matrix interface for Cr-Mo steel. The inhibition of hydrogen entry due to gas nitriding can be explained basically by the two kinds of shielding effects including site competition mechanism. When hydrogen charging is applied on the gas-nitrided specimen, surface nitride layer first prevent the entry of hydrogen (first shielding effect). Even if hydrogen atoms pass through the nitride layer, the lattice diffusion of hydrogen atoms is difficult because nitrogen atoms already exist in interstitial position. In addition, hydrogen atoms are difficult to gather around defects, such as dislocations, grain boundary, and carbide- or nitride-matrix interface because the positions are also occupied by nitrogen atoms (second shielding effect by site competition mechanism).

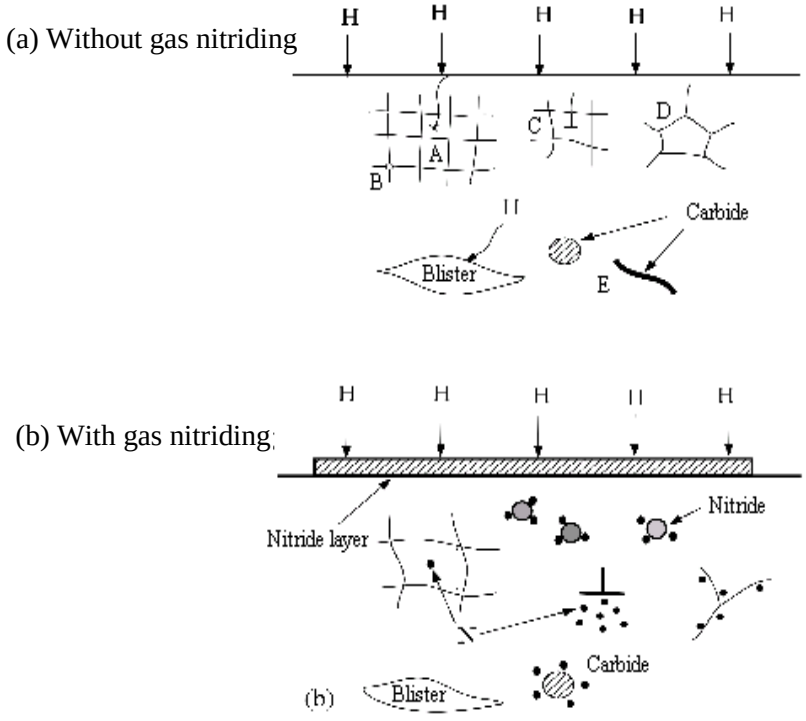

Fig.26 Schematic hydrogen entry, diffusion, trapping and blister formation process in the specimen without gas nitriding (a) and gas nitrided specimen (b).

Chapter 6: Conclusions

The purpose of present research is to investigate the effect of surface treatments on corrosion behavior of different kind of steels in accelerated seashore environment. The conclusions obtained are as follows:

1. Protective rust that can be consider as (natural coat) is being formed with time under laboratory accelerated corrosion test without spraying of Na_2SO_4 solution for both weathering and carbon steel with dripping of either NaCl or $MgCl_2$ solution.
2. TiO_2-coating inhibits the corrosion of the weathering steel by shielding effect and cathodic protection effect in polarization test. In dipping test, the UV-light accelerates the corrosion of weathering steel with or without TiO_2 coat as active oxygen due to the photo-electrochemical reaction promotes the corrosion and rust formation. However in dropping test where the amount of O_2 is high than in dipping, UV-light inhibits the corrosion of both steels due to the promotion of protective nature of the rust.
3. For all kinds of stainless steels with different surface finish Pitting potential in 3% NaCl solution increase with the contents of chromium, molybdenum, and nitrogen. Surface finish is one of the basic parameters in determining the pitting potential. In general, the resistance towards pitting corrosion in 3% NaCl solution is in the following order of No.4 (polishing) > No.2B (Brighten) > No.2D (Dull) and No.1 (Pickled), for austenitic, duplex and ferritic stainless steels as the polishing surface finish has least irregularity and defects, which leads to completion of uniform passive film. The Kelvin probe is one of the tools able to distinguish the existence of the pitting, general corrosion, and passivity.
4. Gas nitride inhibits the corrosion of both weathering steel and Cr-Mo steel due to the shielding effect. Both gas nitride layer and diffusion zone inhibit the hydrogen entry and

delay formation of blister for pure iron and Cr-Mo steel due to the shielding and site competition effects.

ホームページに戻る　→
http://www006.upp.so-net.ne.jp/nakasa/